

# Probing the Magnetic Relaxation and Magnetic Moments Arrangement in a Series of Dy<sub>4</sub> Squares

Jianfeng Wu, Shuang-Yan Lin, Si Shen, Xiao-Lei Li, Lang Zhao, Li Zhang and Jinkui Tang\*

Table S1. Crystallographic data for complexes **1-3**.

	<b>1</b>	<b>2</b>	<b>3</b>
Formula	C <sub>98</sub> H <sub>149</sub> Dy <sub>8</sub> N <sub>11</sub> O <sub>56</sub>	C <sub>54</sub> H <sub>88</sub> Dy <sub>4</sub> N <sub>6</sub> O <sub>23</sub> S <sub>2</sub>	C <sub>52</sub> H <sub>68</sub> Dy <sub>4</sub> N <sub>6</sub> O <sub>23</sub> S <sub>2</sub>
FW, g·mol <sup>-1</sup>	3677.28	1903.42	1859.24
crystal system	Monoclinic	Triclinic	Triclinic
space group	<i>C</i> 2/ <i>c</i>	<i>P</i> - <i>I</i>	<i>P</i> - <i>I</i>
<i>T</i> , K	273(2)	296(2)	273(2)
<i>λ</i> , Å	0.71073	0.71073	0.71073
<i>a</i> , Å	27.3361(9)	10.465(6)	10.1501(6)
<i>b</i> , Å	26.2199(9)	13.832(7)	12.5967(8)
<i>c</i> , Å	22.9128(8)	14.762(8)	13.2679(8)
<i>α</i> , °	90	68.793(9)	87.2500(10)
<i>β</i> , °	92.2230(10)	88.158(11)	82.0570(10)
<i>γ</i> , °	90	68.409(9)	68.6090(10)
<i>V</i> , Å <sup>3</sup>	16410.4(10)	1839.8(16)	1564.38(17)
<i>Z</i>	4	1	1
ρ <sub>calcd</sub> , g·cm <sup>-3</sup>	1.488	1.718	1.974
GOF on <i>F</i> <sup>2</sup>	1.039	1.084	1.105
reflns collected	45670	11398	9792
<i>R</i> <sub>1</sub> ( <i>I</i> ≥ 2 σ( <i>I</i> ))	0.0432	0.0393	0.0445
<i>wR</i> <sub>2</sub> (all data)	0.1355	0.1214	0.1375
CCDC	1432432	1432431	1432430

Table S2. Selected bond distances ( $\text{\AA}$ ) and angles ( $^\circ$ ) for complexes **1**, **2** and **3**.

Complex <b>1</b>	Complex <b>2</b>	Complex <b>3</b>			
Dy(1)-O(1)	2.4855(72)	Dy(1)-O(1)	2.4935(11)	Dy(1)-O(1)	2.4534(4)
Dy(2)-O(1)	2.4902(63)	Dy(2)-O(1)	2.4662(12)	Dy(2)-O(1)	2.5317(4)
Dy(3)-O(1)	2.5056(74)				
Dy(4)-O(1)	2.5274(66)				
Average Dy-O	2.5024(25)	Average Dy-O	2.4798(5)	Average Dy-O	2.4925(5)
Dy(1)-Dy(2)	3.5689(8)	Dy(1)-Dy(2)	3.4922(17)	Dy(1)-Dy(2)	3.5237(6)
Dy(2)-Dy(3)	3.5648(8)	Dy(1)-Dy(2)A	3.5219(19)	Dy(1)-Dy(2)A	3.5272(6)
Dy(3)-Dy(4)	3.5686(8)	Dy(1)-Dy(1)A	4.9870(22)	Dy(1)-Dy(1)A	4.9069(6)
Dy(4)-Dy(1)	3.5657(7)	Dy(2)-Dy(2)A	4.9323(23)	Dy(2)-Dy(2)A	5.0634(6)
Average Dy-Dy	3.5670	Average Dy-Dy	3.5077	Average Dy-Dy	3.5254
Dy(1)-O1-Dy(2)	91.658	Dy(1)-O1-Dy(2)	89.514(21)	Dy(1)-O1-Dy(2)	89.944(12)
Dy(2)-O1-Dy(3)	91.051	Dy(1)-O1-Dy(2)A	90.486(20)	Dy(1)-O1-Dy(2)A	90.056(12)
Dy(3)-O1-Dy(4)	90.289				
Dy(4)-O1-Dy(1)	90.656				
Average Dy-O-Dy	90.914	Average Dy-O-Dy	90	Average Dy-O-Dy	90
Dy(1)-O1-Dy(3)	164.861	Dy(1)-O1-Dy(1)A	180	Dy(1)-O1-Dy(1)A	180
Dy(2)-O1-Dy(4)	166.064	Dy(2)-O1-Dy(2)A	180	Dy(2)-O1-Dy(2)A	180
symmetry code:		A (1-x, 1-y, 1-z)		A (-x, 2-y, 1-z)	

Table S3. Bond valence sum calculations<sup>1</sup> for complexes **1-3** and [Dy<sub>4</sub>(μ<sub>4</sub>-OH)] reported in the literature.

	[Dy <sub>4</sub> (μ <sub>4</sub> -OH)] <sup>ref 25</sup>		Complex <b>1</b>		Complex <b>2</b>		Complex <b>3</b>	
Bond	R	S <sup>a)</sup>	R	S	R	S	R	S
Dy(1)-O(1)	2.506	0.2736	2.485	0.289	2.493	0.283	2.453	0.315
Dy(2)-O(1)	2.500	0.2779	2.490	0.285	2.466	0.304	2.531	0.257
Dy(3)-O(1)	2.513	0.2687	2.505	0.274				
Dy(4)-O(1)	2.529	0.2578	2.527	0.259				
BVS		1.078		1.107		1.174		1.144

S=(R/R<sub>1</sub>)<sup>-N</sup>, R<sub>1</sub>=2.053 and N=6.5 for Dy<sup>3+</sup>.

Table S4. The *CSHM* values calculated by *SHAPE* 2.1 for **1** and  $[\text{Dy}_4(\mu_4\text{-OH})]$ <sup>ref25</sup>.

Coordination Geometry	Complex <b>1</b>				$[\text{Dy}_4(\square_4\text{-OH})]$ <sup>ref25</sup>			
	Dy1	Dy2	Dy3	Dy4	Dy1	Dy2	Dy3	Dy4
Capped square antiprism J10 ( $C_{4v}$ )	2.004	1.875	2.123	1.822	1.920	1.951	1.903	1.966
Spherical capped square antiprism ( $C_{4v}$ )	1.363	1.175	1.424	1.146	1.179	1.218	1.081	1.200
Tricapped trigonal prism J51 ( $D_{3h}$ )	3.630	3.458	3.748	3.252	3.318	3.386	3.057	3.463
Spherical tricapped trigonal prism ( $D_{3h}$ )	1.882	1.785	1.857	1.857	1.875	1.867	2.036	1.788

Table S5. The *CSHM* values calculated by *SHAPE* 2.1 for **2** and **3**.

Coordination Geometry		Complex <b>2</b>	Complex <b>3</b>
Capped square antiprism J10 ( $C_{4v}$ )	Dy1	1.690	1.852
Spherical capped square antiprism ( $C_{4v}$ )		1.064	0.965
Tricapped trigonal prism J51 ( $D_{3h}$ )		1.333	2.268
Spherical tricapped trigonal prism ( $D_{3h}$ )		0.782	0.934
Square antiprism ( $D_{4d}$ )	Dy2	2.501	3.076
Triangular dodecahedron ( $D_{2d}$ )		2.740	2.972
Biaugmented trigonal prism J50 ( $C_{2v}$ )		2.395	2.438
Biaugmented trigonal prism ( $C_{2v}$ )		2.168	3.725

Table S6. Minimal reorientation energies ( $\text{cm}^{-1}$ ) calculated from Magellan program<sup>2</sup> for complexes **1-3**.

	Complex <b>1</b>	Complex <b>2</b>	Complex <b>3</b>
Dy(1)	266.0	Dy(1)	188.8
Dy(2)	289.3	Dy(2)	589.8
Dy(3)	294.7		Dy(2)
Dy(4)	266.2		382.9

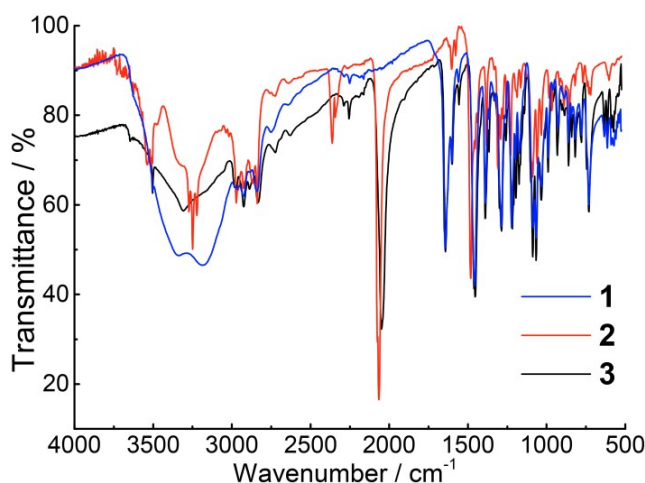


Fig. S1 IR spectra of complexes **1** (blue), **2** (red) and **3** (gray).

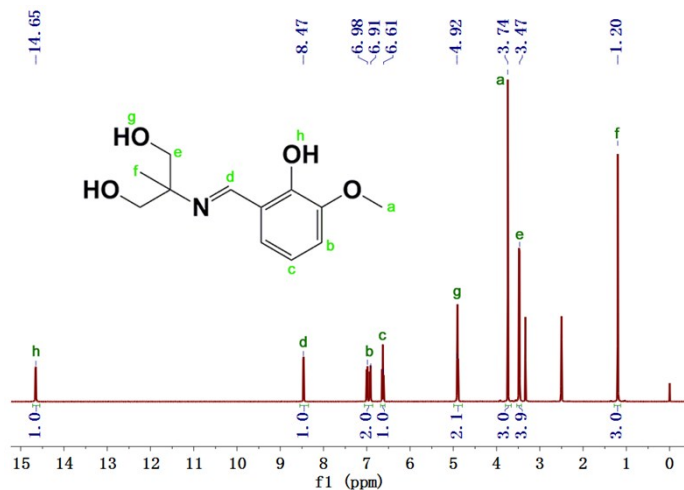


Fig. S2  $^1\text{H}$  NMR spectrum of ligand  $\text{H}_3\text{L}^1$  at 295.0 K (DMSO, 400 MHz).

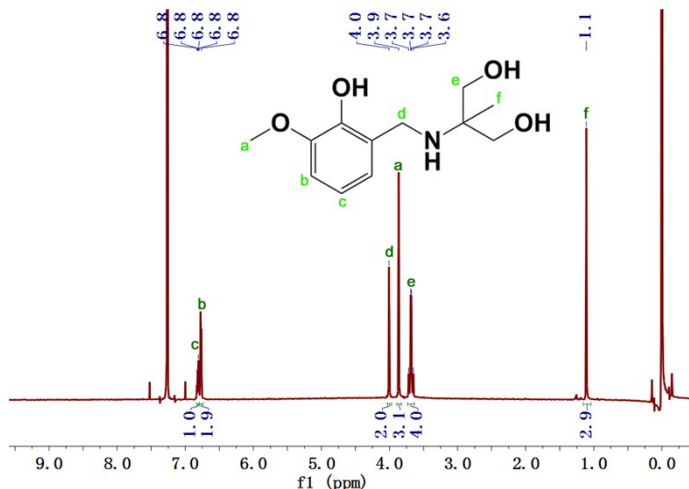


Fig. S3  $^1\text{H}$  NMR spectrum of ligand  $\text{H}_3\text{L}^2$  at 295.0 K ( $\text{DCCl}_3$ , 400 MHz). The active hydrogen atoms are substituted by deuterated reagent.

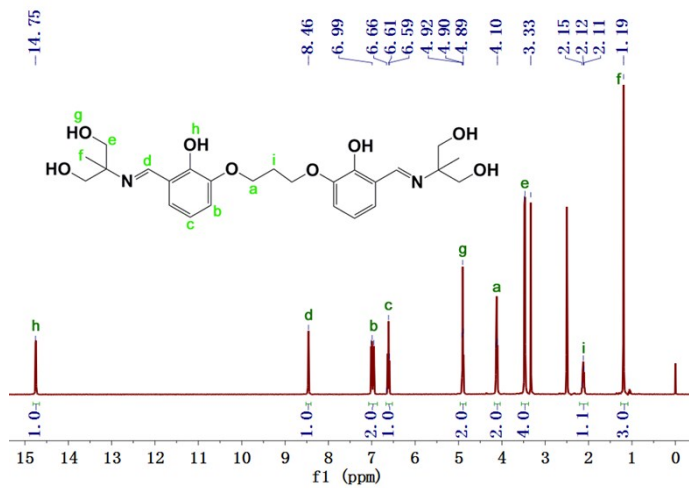


Fig. S4  $^1\text{H}$  NMR spectrum of ligand  $\text{H}_6\text{L}^3$  at 295.0 K (DMSO, 400 MHz).

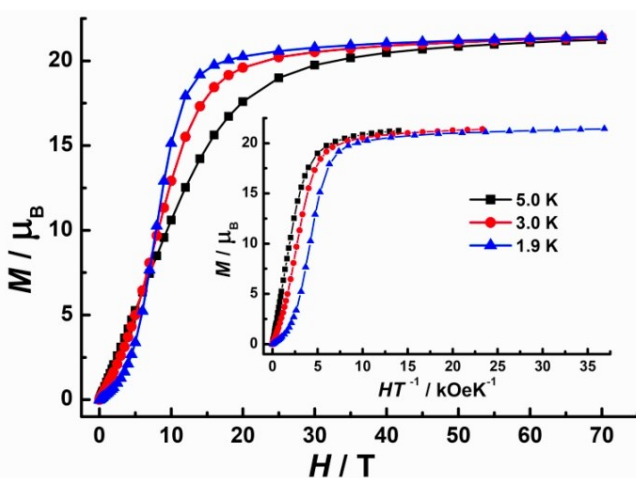


Fig. S5 Molar magnetization ( $M$ ) versus magnetic field ( $H$ ) for **1** at indicated temperature. Inset represents the plots of magnetization  $M$  versus  $H/T$ .

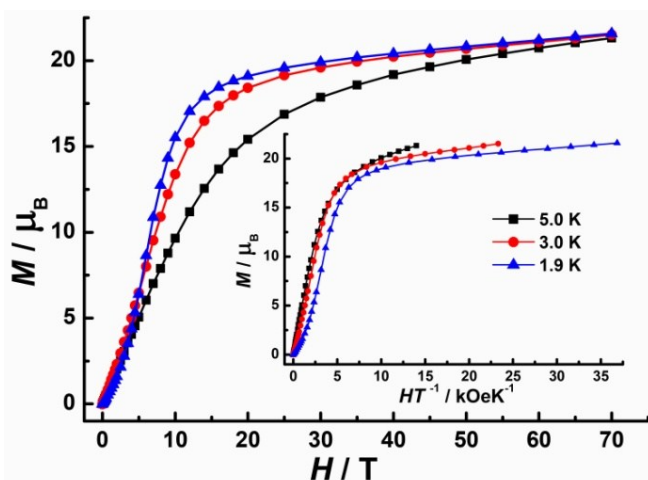


Fig. S6 Molar magnetization ( $M$ ) versus magnetic field ( $H$ ) for **2** at indicated temperature. Inset represents the plots of magnetization  $M$  versus  $H/T$ .

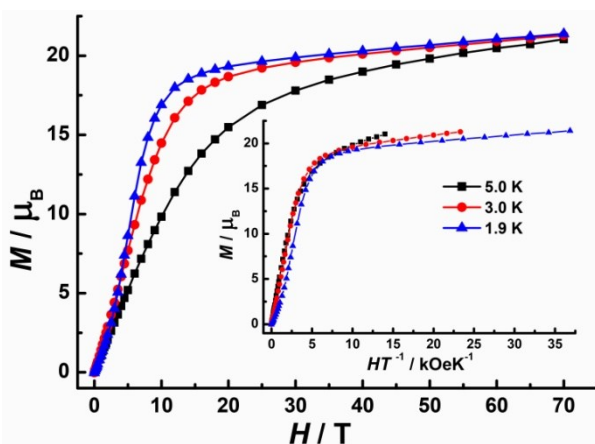


Fig. S7 Molar magnetization ( $M$ ) versus magnetic field ( $H$ ) for **3** at indicated temperature. Inset represents the plots of magnetization  $M$  versus  $H/T$ .

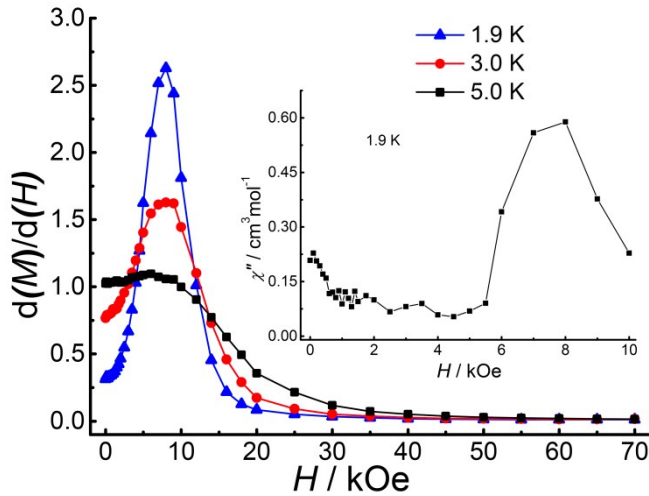


Fig. S8  $d(M/M_s)/dH$  at different temperatures for **1**. Inset represents the plot of field dependent out-of-phase ( $\chi''$ ) susceptibility at 1.9 K.

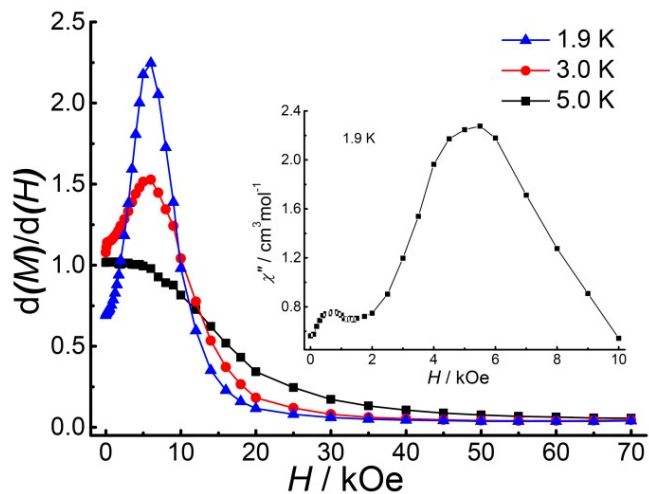


Fig. S9  $d(M/M_s)/dH$  at different temperatures for **2**. Inset represents the plot of field dependent out-of-phase ( $\chi''$ ) susceptibility at 1.9 K.

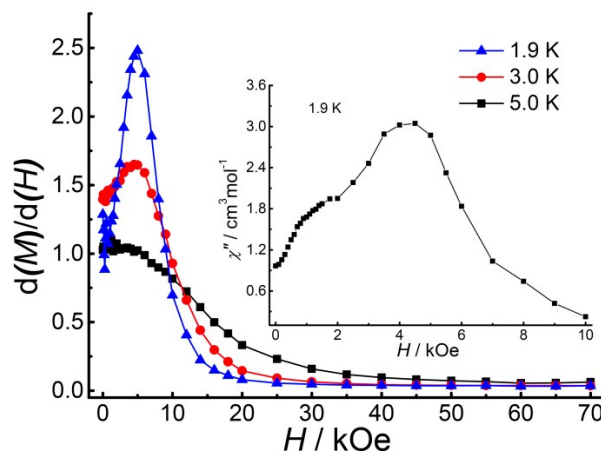


Fig. S10  $d(M/M_s)/dH$  at different temperatures for **3**. Inset represents the plot of field dependent out-of-phase ( $\chi''$ ) susceptibility at 1.9 K.

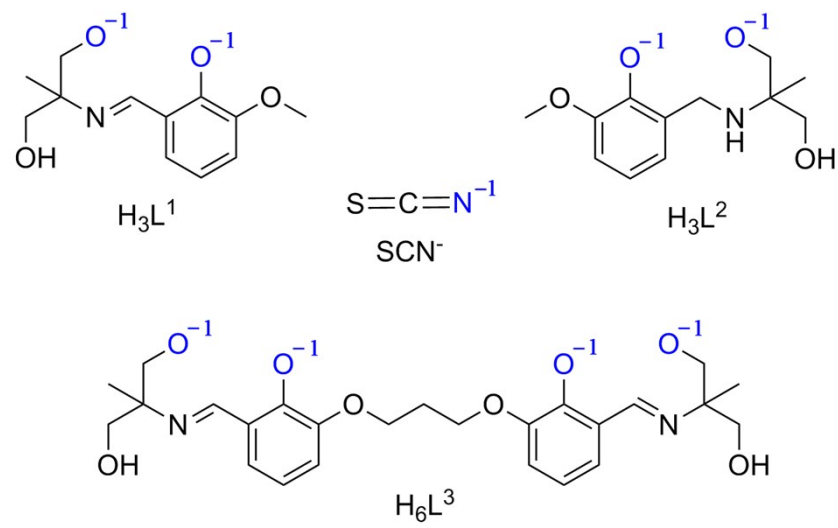


Fig. S11 Partial charges assigned to the formally charged ligands in complexes **1-3**.

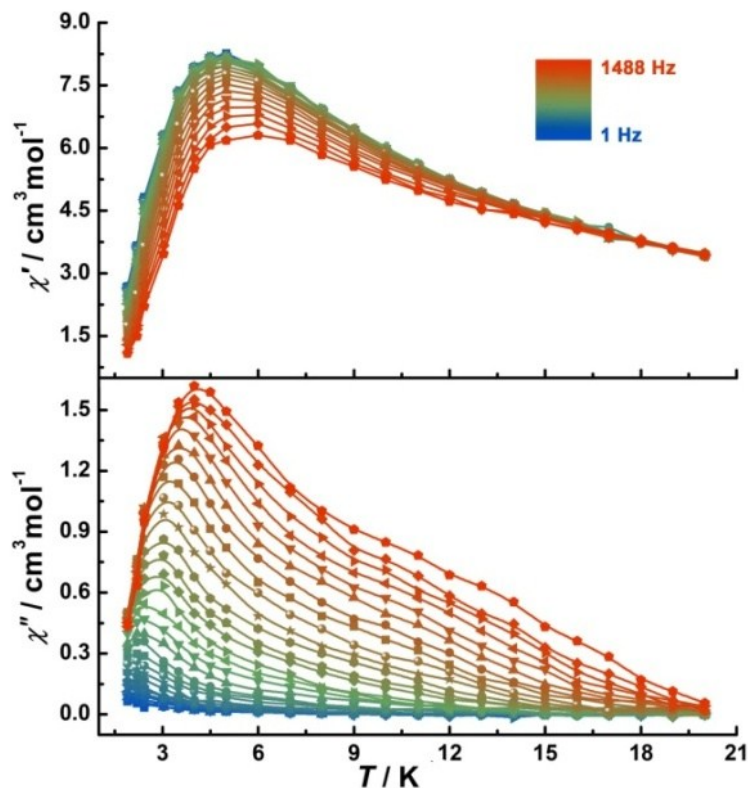


Fig. S12 Temperature dependent ac susceptibility for **1** under zero dc field.

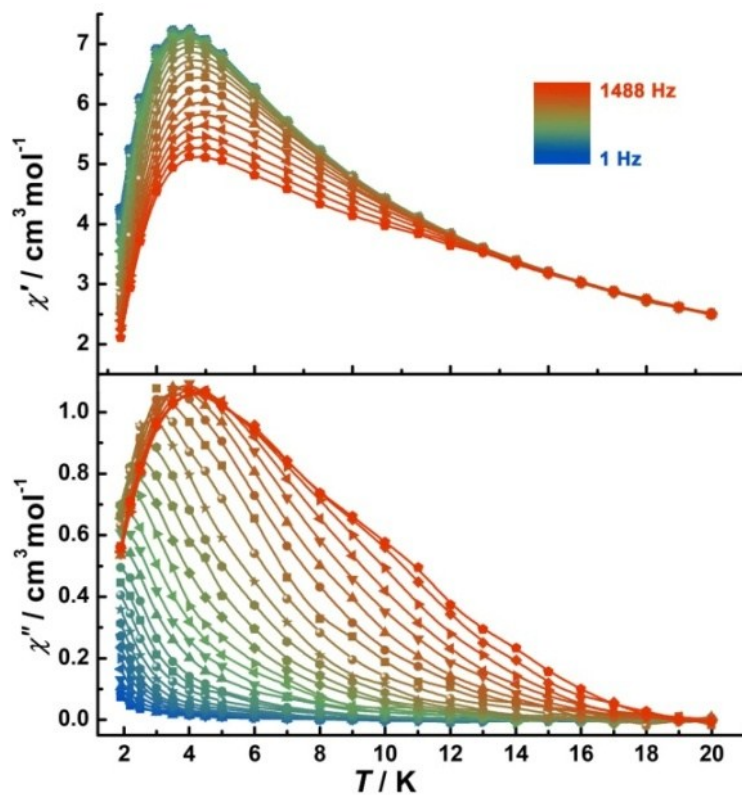


Fig. S13 Temperature dependent ac susceptibility for **2** under zero dc field.

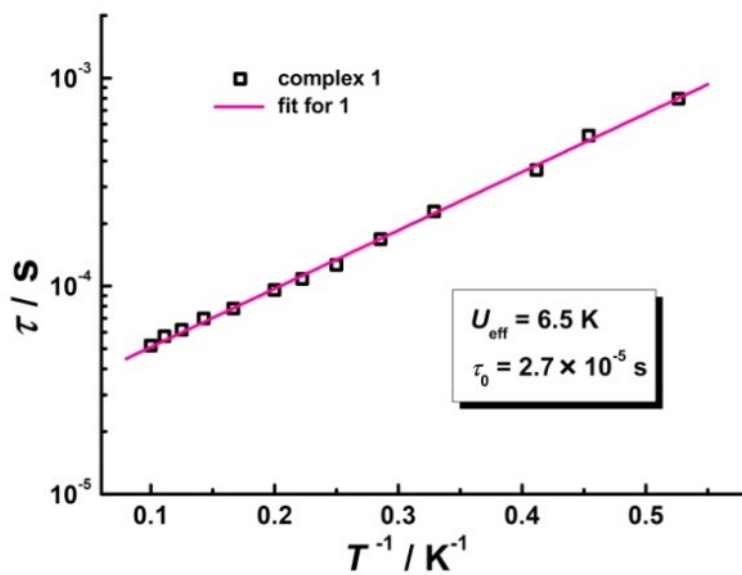


Fig. S14 Plot of  $\tau$  vs.  $T^{-1}$  for **1**. The red line represents the Arrhenius fitted result.

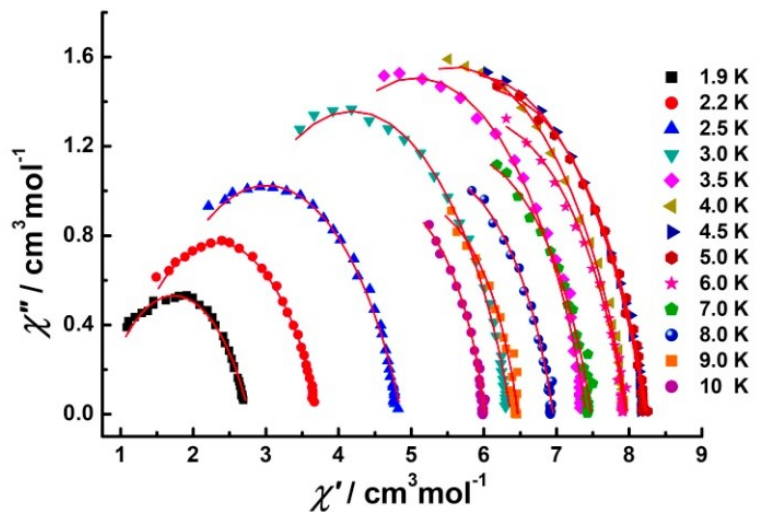


Fig. S15 Cole-Cole plots for **1** under indicated temperature. The solid lines indicate the best fits to the experiments with the generalized Debye model.

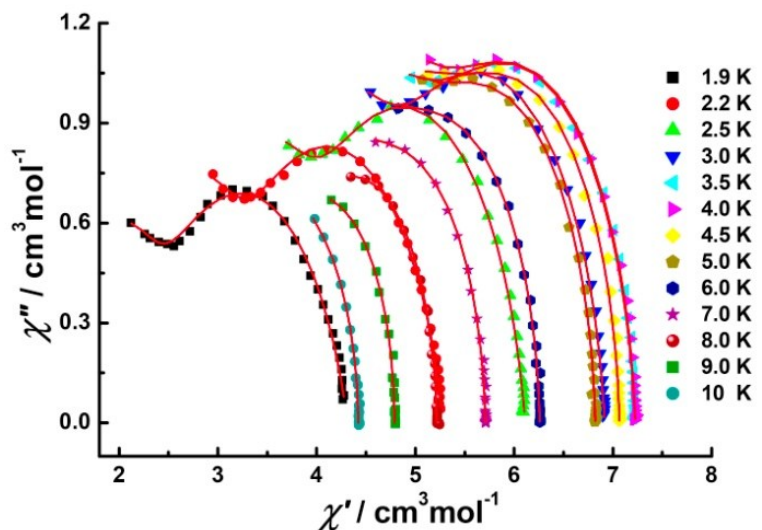


Fig. S16 Cole-Cole plots for **2** under indicated temperature. The solid lines indicate the best fits to the experiments with the double relaxation model.

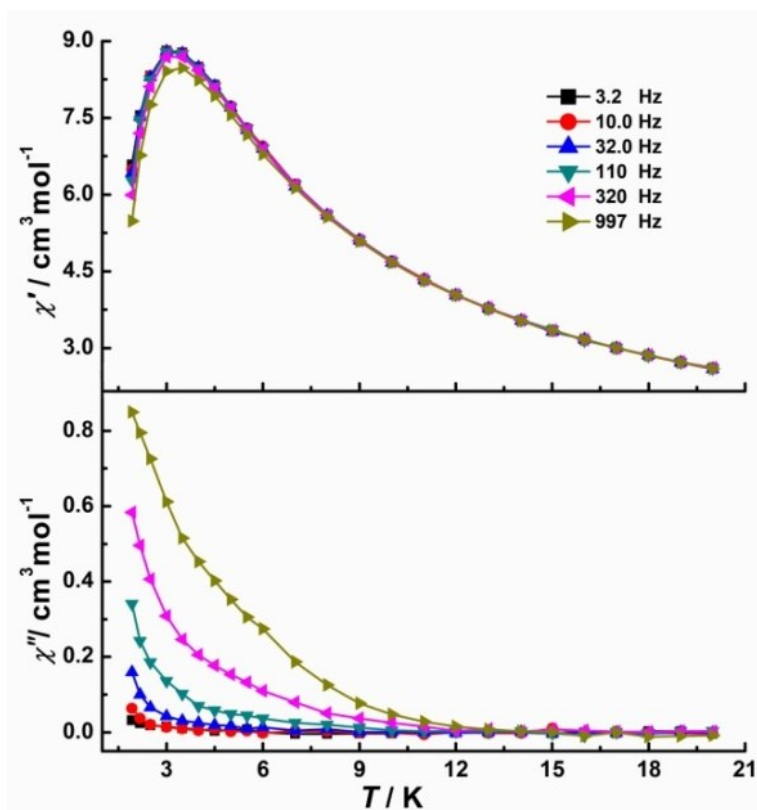


Fig. S17 Temperature-dependent ac susceptibility for **3** at indicated frequency, under zero dc field.

1. I. D. Brown and K. K. Wu, *Acta Crystallographica Section B*, 1976, B32, 1957-1959.
2. N. F. Chilton, D. Collison, E. J. L. McInnes, R. E. P. Winpenny and A. Soncini, *Nat Commun*, 2013, 4, 2551.